PERGAMON

International Journal of Heat and Mass Transfer 43 (2000) 4275–4284

International Journal of HEAT and MASS TRANSFER

www.elsevier.com/locate/ijhmt

Thermal conductivity of suspensions in shear flow fields

Sehyun Shin*, Sung-Hyuk Lee

School of Mechanical Engineering, Kyungpook National University, 1370 Sankyuk-dong, Buk-gu, Taegu 702-701, South Korea

Received 23 March 1999; received in revised form 4 February 2000

Abstract

In the present article, the rheological behavior and the thermal conductivity of suspensions were investigated experimentally by examining the effects of shear rate, particle size, and volume concentration. The thermal conductivity measurements were conducted under rotating Couette flow conditions with a varying rotational speed of the outer cylinder. Homogeneous test suspensions were prepared with uniformly dispersed and neutrally buoyant micro-particles. Four different sizes of plastic particles (25–300 μm) were used as suspended particles. The volume concentrations of the particles and shear rates varied within the ranges of 0–10% and 0–900 1/s, respectively. For the test suspensions, the limiting viscosities at high shear rates were correlated with the Batchelor equation. The highly concentrated suspension in the present study showed the shear thinning viscosity. The thermal conductivities measured at stationary condition showed excellent agreements with values in saturated water table and were correlated satisfactorily with the Brailsford–Major equation. The thermal conductivity of the test suspensions in shear flow increased with shear rate and displayed asymptotic plateau values at high shear rates. The shear-rate-dependent conductivity was strongly affected by both particle size and volume concentration in shear flow field.

1. Introduction

Understanding the flow and heat transfer behavior of suspensions becomes increasingly important as the application of suspensions extends to various areas such as paints, composite materials, ceramics, electronic industry, polymers, and so on. Recently, there has been a new interest in obtaining more quantitative information and behavioral understanding related to suspensions in order to use them more effectively in practical applications. However, when dealing with a practical engineering problem concerning a suspension, the heat transfer cannot be easily estimated even in a simple geometry like a circular duct. One of the main reasons is that the viscosity and thermal conductivity of the suspension vary with both shear rate and temperature, thereby significantly influencing the heat transfer performance. In order to successfully apply suspensions in heat transfer equipment, one needs to have a better understanding of their thermal transport characteristics and thermal properties.

Generally, the flow of a particle dispersion shows a non-Newtonian behavior even though the particles are suspended in Newtonian medium [1]. Moreover, the deviation from the Newtonian flow behavior becomes pronounced under strong shear flow fields. When the particle volume concentration is low, the suspension behaves like a Newtonian fluid as the medium solvent [2–4]. However, as the particle concentration increases, non-Newtonian behavior is observed such as shear thinning and high-shear-rate

* Corresponding author. Tel.: +82-53-950-6570; fax: +82-53-956-9914.

E-mail address: shins@kyungpook.ac.kr (S. Shin).

0017-9310/00/$ - see front matter
PII: S0017-9310(00)00050-8

Nomenclature

a	particle radius
d	particle diameter
D	gap between two cylinders
k	thermal conductivity
l	cylinder length
n	exponent for a power-law relationship
Q	heat rate (W)
r	radius of cylinder
T	temperature (refer to subscript section)
u	velocity component
$\dot{\gamma}$	shear rate
Φ	particle volume fraction
κ	Boltzmann constant
ω	rotational speed

Greek symbols

ρ	density

Subscripts

L	liquid phase
i	inner cylinder
o	outer cylinder
p	particle
0	zero/stationary
∞	ambient/infinite

limiting viscosity. The rheological behavior of dilute particle dispersion was pioneered theoretically by Einstein [2], and thereafter, the applicable range of particle loading was extended to a concentrated suspension by Batchelor [3] and Jeffrey and Acrivos [4].

When the flow of a particle dispersion is imposed on thermal load, its thermal behavior deviates from that of Newtonian fluid. Similarly, the deviation from Newtonian thermal behavior becomes pronounced under strong flow fields and at high volume concentration. Several researchers have reported the effect of shear rate on the thermal conductivity of suspensions, but their results are inconclusive. Ahuja [5] measured the thermal conductivity of polystyrene suspensions including microparticles of polystyrene (50–100 μm) in a neutrally buoyant fluid. Since his measurements were taken in a concentric axial flow, the shear rate distribution was not completely uniform, and thus it is difficult to compare his results with others. Sohn and Chen [6] measured the thermal conductivity of polyethylene suspensions under low-velocity and Couette flow conditions. They reported that when the particle Peclet number was sufficiently high, the thermal conductivity increased with increasing shear rate.

Sohn and Chen [7] also analytically investigated the effect of shear-rate-dependent thermal conductivity on the heat transfer behavior of suspensions. The increased thermal conductivity was explained by the theory that the rotation of particles in a shear flow field induced the so-called micro-scale convection. This concept of micro-convection can be helpful in understanding the mechanism of increased thermal conductivity in suspensions. Charunyakorn et al. [8] analytically investigated the heat-transfer enhancement of a slurry flow using a micro-encapsulated phase-changematerial. They predicted heat transfer behavior using the shear-rate-dependent thermal conductivity for the slurry.

More recently, Lee and Irvine [9], who used a rotating coaxial cylinder system, reported that a non-Newtonian fluid displayed a shear-rate dependence on both viscosity and thermal conductivity of carboxymethylcellulose (CMC) and polyacrylamide (Separan AP-273) solutions. However, the increase in thermal conductivity relative to shear rate was greater with low concentration solutions than with high-concentration solutions — a phenomenon that cannot be explained. Therefore, the objective of the present study was to measure the thermal conductivity of various suspensions under steady conditions over a range of shear rates with rheological property.

2. Preparation of suspensions and viscosity measurements

2.1. Preparation of test suspensions

Polyethylene and polypropylene particles were chosen as the dispersed particles for the present study. The mean diameters of the three polyethylene particles selected were 25, 100, and 180 μm, while that of the polypropylene particles was 300 μm. In the case of the 25 μm particles, the actual size varied from 5 to 30 μm, peaking at 25 μm. Also, the actual deviations in the diameter for the other three cases were approximately 100 ± 10 μm, 180 ± 20 μm, and 300 ± 20 μm, respectively. Other physical properties of the particles are shown in Table 1.

A liquid mixture consisting of silicon oil and kerosene was used as the suspending liquid medium. Since the density difference between the particles and the dis-

Table 1
Properties of test suspensions

	Silicon oil (S)	Kerosene (K)	Suspension I	Suspension II	Suspension III	Suspension IV
Particle size (μm)	–	–	25	100	180	300
Mixing ratio (S:K)	–	–	66.2:33.8	66.2:33.8	80.3:19.7	44.0:56.0
ρ (kg/m^3)	975	797.4	915	915	940	876
k (W/m K)	0.164	0.150	0.159	0.159	0.163	0.156
c_p(J/kg K)	1736.1	2249.6	1909.6	1909.6	1828.5	2023.7
μ(mPa s)	908	1.225	148	148	314	38
Re_p	–	–	5.08×10^{-4}	8.14×10^{-3}	1.28×10^{-2}	3.11×10^{-1}

persed liquid should be kept as small as possible to prevent the separation of the particles in the suspending liquid medium, the density of the suspending fluid was adjusted to that of a given particle by mixing a proper amount of silicon oil with kerosene in the present study. No possible sedimentation or floating of the particles was observed for 3–4 days. Hence, the Brownian motion effect can be assumed to be negligible in the present study. Also, particle inertia effect is neglected since the particle Reynolds number $Re_p = \rho_L \dot{\gamma} a^2/\eta_L$ ranges from 10^{-4} to 10^{-1} as listed in Table 1. Finally, the particle volume concentration was varied from 2% to 10% in the present suspensions.

The viscosity of the suspensions was measured over a wide range of shear rates with a HAAKE viscometer and Brookfield viscometer under a steady shear flow. The temperature was fixed at 298 K. In the investigation of the suspension rheology, the volume concentration, defined as the volume fraction of the total suspension occupied by suspended particles, is often used instead of mass concentration. One of the reasons why the volume concentration is used is that suspension rheology greatly depends on the hydrodynamic forces acting on the surface of the particles. In the present study, the volume concentration was determined from the mass concentration of the suspension by the following equation:

$$\Phi_v = \frac{1}{1 + \dfrac{1 - \Phi_m}{\rho_L}\dfrac{\rho_p}{\Phi_m}} \tag{1}$$

where ρ_p and ρ_L are the densities of the particles and suspending liquid, respectively, and Φ_v and Φ_m are the volume and mass concentrations (%) of the suspension, respectively. As indicated in the above equation, the densities of the particles and suspending liquid are the same so that the volume concentration (Φ_v) is equivalent to mass concentration (Φ_m) of the suspension in the present study. Prior to measuring the viscosity of the test suspensions, calibration runs were conducted with distilled water and a standard-viscosity fluid (4.3 mPa s at 298 K) supplied by the manufacturer of the Brookfield viscometer.

2.2. Rheological behavior at various concentrations

For dilute suspensions, Einstein [2] and Batchelor [3] determined theoretically the first (Φ) and the second (Φ^2) order correlations, respectively, to the relative viscosity.

$$\eta/\eta_L = 1 + 2.5\Phi + 6.2\Phi^2 \tag{2}$$

Here, η and η_L represent the viscosities of the suspension and the solvent, respectively. In Fig. 1, the high-shear-limiting viscosities are plotted as a function of the particle volume concentrations. Also, included for comparison are the predictions from the correlations of Einstein and Batchelor. As expected in this plot, the viscosity of the prepared suspension was in good

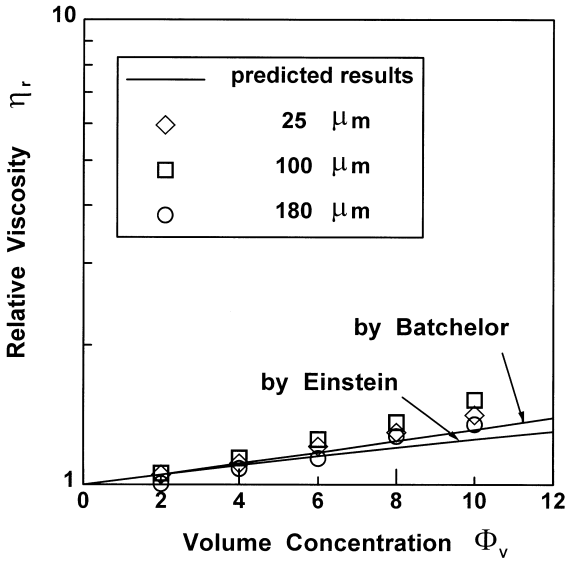

Fig. 1. Relative high-shear-rate limiting viscosity as a function of the particle volume concentration at 298 K. Lines for predictions from theories of Einstein and Batchelor.

agreement with those predicted by Einstein's and Batchelor's models for the test suspension.

In Fig. 2, the relative suspension viscosities are plotted as a function of a reduced shear stress $\tau_r = \tau a^3/\kappa T$, where τ is the shear stress, a is the radius of particle, κ is the Boltzmann constant, and T is the absolute temperature. Also included for comparison is the volume concentration effect on the relative viscosity in the range of $\Phi = 0$–10%. The superposition of results for different particle size suspensions falls on a single curve for fixed volume concentrations similar to the previous results [4]. The deviation could be attributed to the polydisperse particles in the present suspensions. Each curve for different concentrations showed a very weak shear thinning viscosity with increasing shear stress.

3. Description of experimental apparatus

3.1. Apparatus

A schematic illustration of the present experimental apparatus is shown in Fig. 3. The experimental apparatus included a rotating mechanism, a constant-temperature water jacket, a constant-temperature water bath, and measurement devices. Thermal conductivity was measured over a wide range of shear rates under rotating Couette flow conditions. Each measurement was conducted at a uniform shear rate. Fig. 4 illustrates the detail of the rotating mechanism. As shown in Fig. 4, the rotating mechanism consists of a coaxial cylinder system in which the inner cylinder is stationary and the outer cylinder is rotating. The detailed tube dimensions and materials of the apparatus are as follows: The inner cylinder was made of aluminum tube with a 48 mm o.d., 61.8 mm length, and 3.85 mm thickness. The outer cylinder was also made of aluminum tube with a 55 mm o.d., 110 mm length, and 2 mm thickness. The test fluid was located in the annular gap of 1.5 mm between the two cylinders. Thus, a plane Couette flow was established between the two cylinders since the gap was sufficiently small compared with the radius of the inner cylinder.

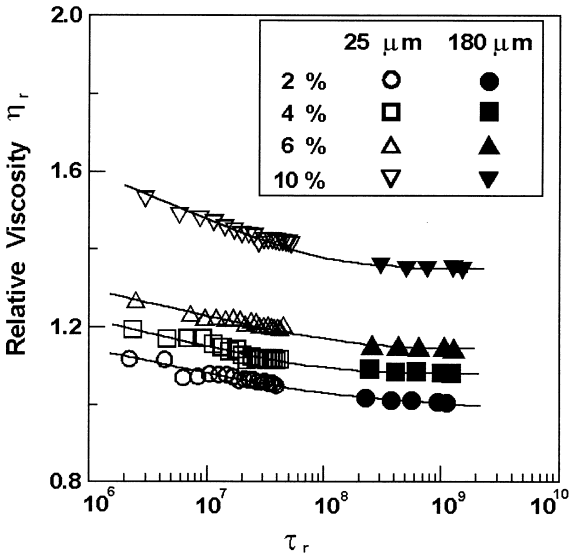

Fig. 2. Relative viscosities of suspensions as function of reduced shear stress for various volume concentrations. Each curve combines data for two different particle sizes of suspension and shows a very weak shear thinning behavior.

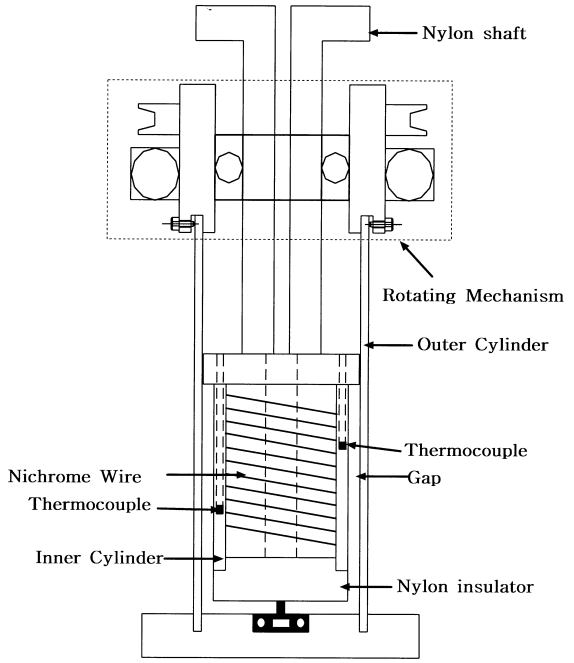

Fig. 3. Detail view of thermal conductivity cell.

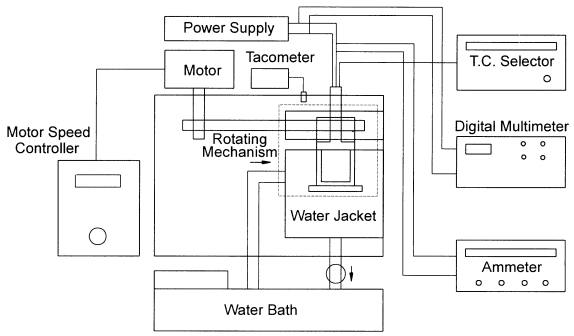

Fig. 4. Schematic of overall experimental setup for thermal conductivity measurement.

The inner cylinder consisted of a thermal probe containing a heating coil. Heat flowed in a radial direction through the test fluid medium in the gap to the outer cylinder. The temperature difference across the gap was approximately 8°C. The dual cylinder assembly was placed in a constant-temperature water bath to maintain the outer cylinder at a known and constant temperature. It is of note that a thermal probe cannot be mounted on the surface of the rotating cylinder. The temperature of the outer cylinder can be assumed to be as the same as that of the water bath when the convective heat transfer coefficients on the surface of the outer cylinder are significantly large.

Thus, the present study adopted multi-water jet system, where water impinged onto the outer surface of the rotating outer cylinder to generate high convective heat transfer coefficients. The performance of the multi-water jet system was carefully examined for various rotating speeds of the outer cylinder. It is of note that while the outer cylinder is stationary (i.e., zero rotating speed), thermocouples can be directly mounted on the surface of the outer cylinder. Three thermocouples were mounted on the surface of the outer cylinder at a stationary condition and the wall temperature was directly measured. Comparing the directly measured temperature with the estimated one from the circulating water, the temperature difference was less than 0.1°C. This result implies that the jet impingement system provides significantly high heat transfer coefficients in the present experimental system such that the outer surface temperature of the outer cylinder can be assumed to be the same as that of the circulating water within 0.1°C of error. The above assumption is even more satisfactory as the rotational speed increases, since the heat transfer rate increases with increasing rotational speed such that the temperature difference between the wall and fluid becomes almost negligible. During the experiments, the temperature fluctuations in the water bath were less than 0.05°C.

Meanwhile, for the inner cylinder, temperatures were measured using two T-type thermocouples. The calibrated thermocouples were painted with silicon paste and inserted into the holes in the inner cylinder wall at two axial locations of two different depths but at the same radial position to determine the axial temperature distribution in the wall of the inner cylinder.

3.2. Mathematical description of a rotating couette flow

In designing the present experimental apparatus, it was necessary to consider the governing equations for a rotating Couette flow with a power-law fluid including viscous dissipation and gap shear-rate variation. It is commonly assumed that there is no radial velocity and hence no radial mean convection in a rotating Couette flow system like the system used here. Therefore, the steady-state energy equation in the rotating Couette flow field is as follows:

$$\frac{1}{r}\frac{\mathrm{d}}{\mathrm{d}r}\left(kr\frac{\mathrm{d}T}{\mathrm{d}r}\right)+\mu\left(\frac{\mathrm{d}u_\theta}{\mathrm{d}r}-\frac{u_\theta}{r}\right)^2=0 \tag{3}$$

If it is assumed that both viscous dissipation and shear rate variation in the gap are negligible, then the thermal conductivity can be determined from the above equation as follows:

$$k(\dot{\gamma})=\frac{Q ln(r_\mathrm{o}/r_\mathrm{i})}{2\pi l(T_\mathrm{i}-T_\mathrm{o})} \tag{4}$$

where

$$\dot{\gamma}=\left[r\frac{\mathrm{d}}{\mathrm{d}r}\left(\frac{u_\theta}{r}\right)\right]=\frac{C_1}{r^{2/n}} \quad \text{and}$$

$$u_\theta=r_\mathrm{o}\omega_\mathrm{o}\frac{(r/r_\mathrm{i})-(r_\mathrm{i}/r)}{(r_\mathrm{o}/r_\mathrm{i})-(r_\mathrm{i}/r_\mathrm{o})}$$

Thus, the measurements required to determine the thermal conductivity in Eq. (4) include the inner wall temperature (T_i), outer wall temperature (T_o), applied heat rate (Q), angular velocity of the outer cylinder (ω_o), cylinder length (l), and radius ratio of outer cylinder to inner cylinder ($r_\mathrm{o}/r_\mathrm{i}$).

3.3. Uncertainty analysis

The effect of viscous dissipation in both Newtonian and non-Newtonian fluids can cause significant errors in the measurement of suspension thermal conductivity. The second term in Eq. (3) represents viscous dissipation, whose magnitude can be represented by a Brinkman number defined for a power-law fluid as:

$$\mathrm{Br}=\frac{K(r_0\omega_0)^{n+1}}{2k_0r_\mathrm{i}^{n-1}(T_\mathrm{i}-T_0)} \tag{5}$$

where K is power-law fluid consistency and k_0 is zero shear-rate thermal conductivity. In general, temperature profiles depend on the Brinkman number. However, if the Brinkman number approaches zero, the viscous dissipation term is negligible. Note that the viscous heating effect for Newtonian fluid is proportional to the square of rotating speed. Brinkman numbers were calculated over the operating region of the present experiments and found to be about 10^{-4}–10^{-1}. Therefore, the effect of viscous dissipation was neglected in the present study.

If free convection exists between the two vertical cylinders, the thermal conductivity measurements will include errors due to the convective heat transfer. As reported by Eckert and Carlson [10] and Elder [11],

the buoyancy-driven velocities in vertical slots for relatively low Rayleigh numbers ($Ra < 1000$) are so small that their geometry does not affect heat transfer. In the present experiment, the maximum Rayleigh number occurred with the lowest viscosity fluid case (i.e., distilled water). Therefore, free convection effects were not expected.

Two calibrated T-type thermocouples were used to measure the temperature of the inner cylinder and were calibrated against a standard platinum RTD. The maximum temperature deviations from the two thermocouples were 0.017 and 0.015°C, respectively. During the experiments, the two thermocouples were checked, and the maximum temperature difference between them was 0.1°C. These temperature measurement errors were considered in the error analysis of the measured thermal conductivity.

The uncertainty due to indirect temperature measurement of the rotating cylinder with the auxiliary water impinging system was less than 0.1°C, as described in earlier section. Other possible uncertainties, including heat loss from a heating coil, the eccentricity of the cylindrical annulus, a secondary flow associated with the Taylor number, and shear-rate measurement were described elsewhere [9,12]. A complete error analysis for the present measurement was conducted and reported by Lee [12]. The total uncertainty of the thermal-conductivity measurement was 4.59%, whereas that of the shear-rate measurement was 8.23%. However, as stated in the following section, calibration runs for the thermal-conductivity-measurement apparatus suggested that the thermal-conductivity uncertainty might be less than the calculated one.

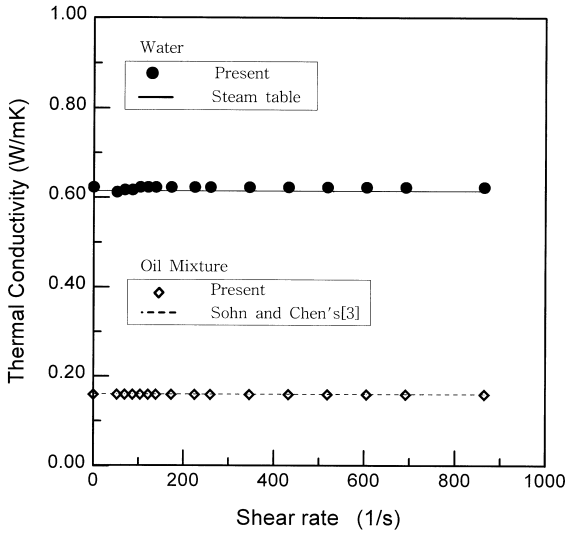

Fig. 5. Thermal conductivity vs. shear rate for distilled water and oil mixture at 298 K.

4. Experimental results and discussion

Prior to measuring the thermal conductivity of suspensions, a series of calibration runs were conducted with distilled water and a standard oil mixture (0.162 W/mK at 298 K) in order to validate the apparatus. Fig. 5 shows the results of the distilled water and oil mixture measurements. The thermal conductivity measured for distilled water showed an excellent agreement with the steam table values [13] within 1% over the shear rate range of interest. This indicated that there was no free convection or shear rate effect on the thermal conductivity measurement of water using the present apparatus. In addition, Fig. 5 shows the thermal conductivity of the mixed oil (silicon oil 66.2% + kerosene 33.8%) at 298 K with varying shear rates. This also showed an excellent agreement with the reported values of Sohn and Chen [6].

Fig. 6 shows the thermal conductivity vs. shear rate curves for suspensions made of 25-, 100-, 180-, and 300-μm particles for six different concentrations, respectively. The results in Fig. 6(a) for 25-μm particles clearly demonstrateis that there was no effect of volume concentrations, even at 10%, on the thermal conductivity when the particle size was small. It is important to note that the thermal conductivity of the particles is larger than that of the liquid mixture. Accordingly, as the volume-concentration of the dispersed particles increases, one can expect that the thermal conductivity increases.

Fig. 6(b) presents the thermal conductivity vs. shear rate curves for suspensions made of 100-μm particles for various concentrations. These curves are distinctly different from those in Fig. 6(a) and showed that the thermal conductivity increased linearly with shear rate in a shear rate range between 50 and 220 1/s, as reported by Sohn and Chen [6]. It is interesting to note that there were both zero- and infinite-shear thermal conductivities. Thermal conductivity was independent below a certain shear rate (i.e., 50 1/s), called zero-shear-rate thermal conductivity. At shear rates greater than 220 1/s, the thermal conductivity reached a plateau value, called infinite-shear thermal conductivity. This infinite-shear thermal conductivity has not been observed in previous experiments. Previously proposed thermal conductivity models [5,6] for suspensions indicated that the thermal conductivity continued to increase with shear rate, a phenomenon which may cause an overestimation of the heat transfer rate for high shear flows. Therefore, having the thermal conductivity values at high shear rates for various suspensions is of vital importance.

The suspensions made of 180- and 300-μm particles were examined by varying shear rates from 0 to 880 1/s, and the results are presented in Fig. 6(b) and (c), respectively. The general trends and characteristics of the thermal conductivity curves are similar to those in Fig. 6(b). The curves in Fig. 6(c) and (d) indicate that the thermal conductivity of the suspensions made of large particles strongly depends on shear rate. This degree of shear-rate dependence increased with the dispersed-particle size.

Based on these test results, we have attempted to obtain a new shear-rate-dependent thermal conductivity model of suspensions. Previous models [5,6] had drawbacks and limits in generalization. For example, the thermal conductivity continues to increase with shear rate [6], a phenomenon which can not occur in

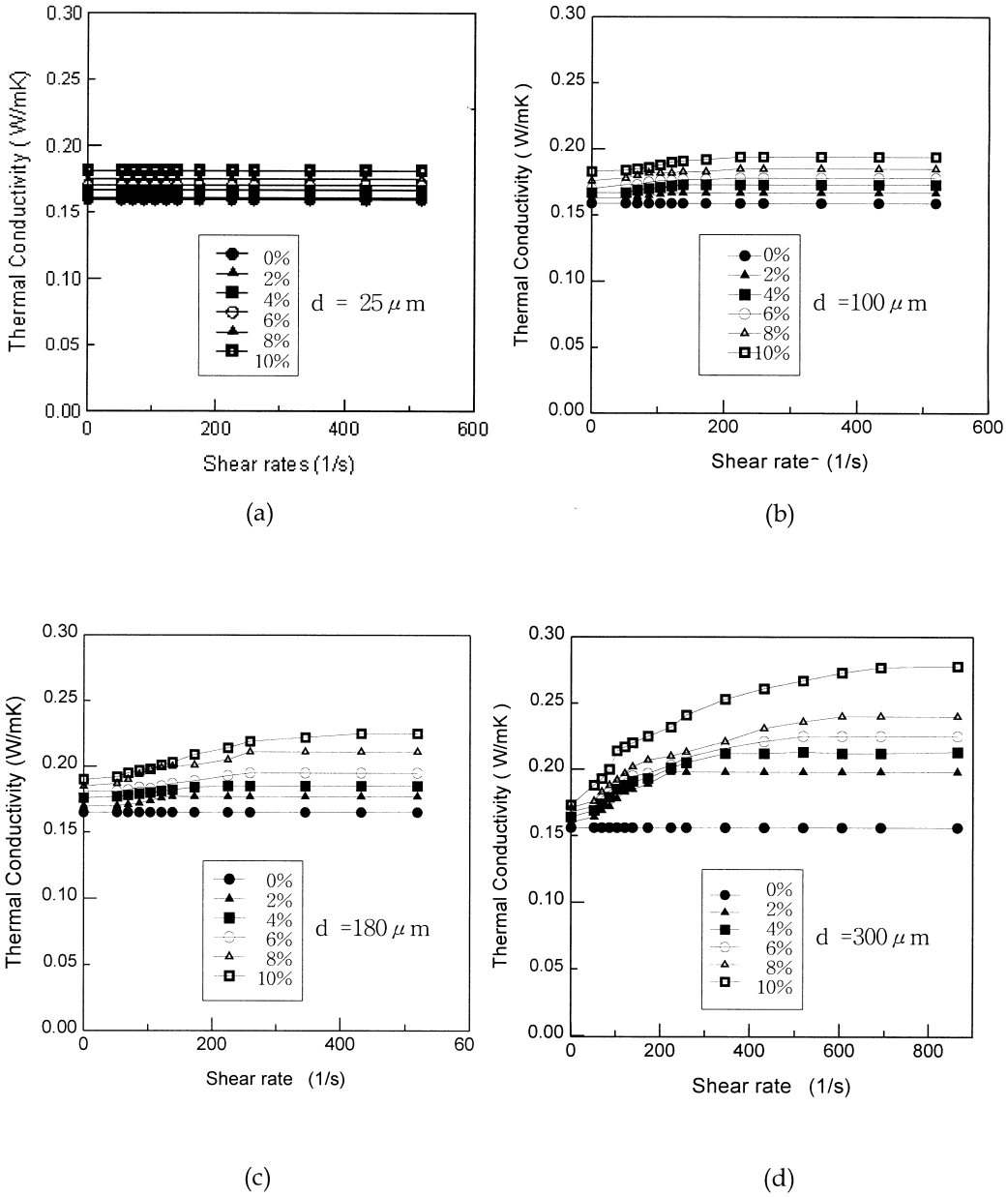

Fig. 6. Thermal conductivity vs. shear rate for the suspensions made of 25-, 100-, 180-, and 300-μm diameter dispersed particles at different volume concentrations.

reality. The presented results demonstrated that suspension thermal conductivity was strongly dependent of several parameters, including the concentration and particle diameter. The present study analyzes the influence of each parameter on the shear-rate-dependent thermal conductivity of suspensions.

The thermal conductivity of suspensions was measured at a zero-shear rate, whose value is called a zero-shear thermal conductivity (k_0). The zero-shear thermal conductivity (k_0) increases with volume concentration of suspended particleis as shown in Fig. 6. Fig. 7 shows the dependence of the thermal conductivity in a stationary state (i.e., zero-shear rate) on volume concentration comparing with previous models [14,15]. For convenience, the relative thermal conductivity in Fig. 7 is defined as the ratio of the thermal conductivity of a fluid with suspended particles to that of the base fluid. In Fig. 7, the zero-shear-rate thermal conductivity of the test suspensions shows a good agreement in the stationary state with the predicted results of Brailsford and Major [14] and Litchnecker [15]. Therefore, the zero-shear thermal conductivity (k_0) can be determined by either of them. The Brailsford–Major correlation is described in the following equation:

$$k_0 = \frac{k_L\Phi_L + k_p\Phi_p\left[3k_L/\left(2k_L + k_p\right)\right]}{\Phi_L + \Phi_p\left[3k_L/\left(2k_L + k_p\right)\right]} \tag{6}$$

where subscripts L and p represents liquid and particle, respectively.

The thermal conductivity starts to increase with shear rate beyond a certain shear rate, which is called a zero-shear rate ($\dot{\gamma}_0$). Fig. 8 shows a relative thermal conductivity vs. shear rate for suspensions made of four different size particles for a fixed volume concentration (10%). The relative thermal conductivity (k/k_0) in Fig. 8 is defined as the ratio of shear-rate-dependent thermal conductivity to zero-shear thermal conductivity. Fig. 8 shows that the thermal conductivity is strongly dependent on the size of the dispersed particles. The larger the particle diameter and volume concentration, the smaller the zero-shear rate. The zero-shear rates were determined for various suspensions with curve-fitting data, resulting in values between 10 and 40 1/s. The present values of zero-shear rates are somewhat lower than those measured by Lee and Irvine [6], who reported that the thermal conductivity of non-Newtonian fluids started to increase at shear rates above 80–100 1/s.

As mentioned earlier, the infinite-shear thermal conductivity was observed beyond a relatively high shear rate, above which the thermal conductivity shows a constant plateau value. Now, it is necessary to correlate the infinite shear rate with other parameters. As shown in Fig. 6, the infinite-shear rates increased as the particle size and concentration increased. It was found that for the suspensions of fixed size particles, the infinite-shear rate was proportional to the volume concentration. For a fixed volume concentration, the infinite-shear rate was proportional to the 1.5th power of non-dimensional particle diameter (i.e., d/D). Fig. 9 shows a correlation curve of the infinite shear rate with both the volume concentration and particle diameter, showing a good agreement with the present exper-

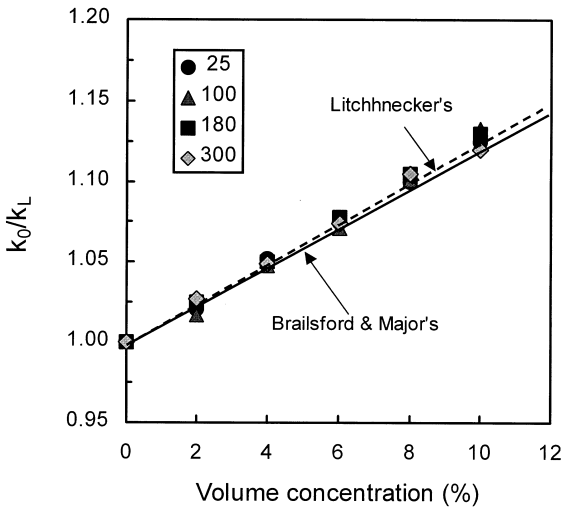

Fig. 7. Relative thermal conductivity at zero-shear rate as a function of particle volume concentration for different particle sizes.

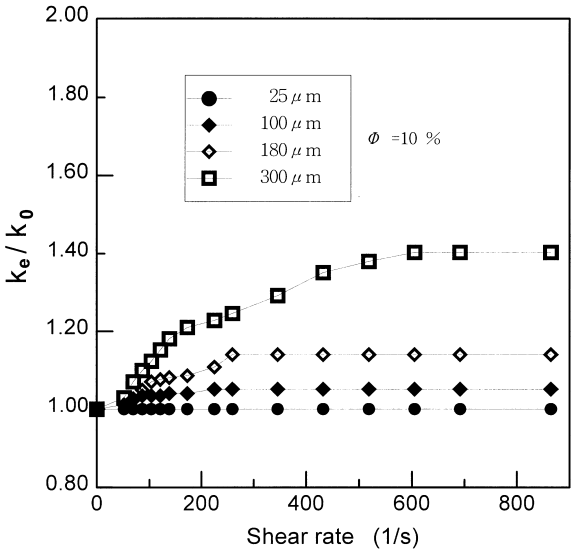

Fig. 8. Relative thermal conductivity vs. shear rate for a fixed volume concentration of 10% at different particle sizes.

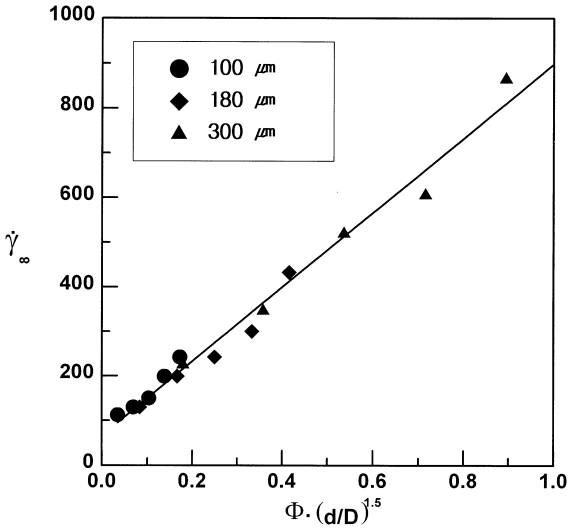

Fig. 9. Infinite-shear rate of the limiting thermal conductivity vs. the abscissa $(\Phi)\ (d/D)^{1.5}$.

imental data. Thus, the present study proposes the following correlation for the infinite-shear rate:

$$\dot{\gamma}_\infty = C_1 + C_2\left[\Phi\left(\frac{d}{D}\right)^{1.5}\right] \tag{7}$$

where $C_1 = 66.42$, $C_2 = 831.9$, and Φ is the volume concentration.

Next, we attempt to correlate the plateau values of the thermal conductivity, i.e., the infinite-shear thermal conductivity (k_∞), with both volume concentration and particle size. It is worth recalling that the zero-shear thermal conductivity (k_0) is a function of the volume concentration only. It was found that the infinite-shear thermal conductivity (k_∞) was dependent on both volume concentration and particle size. Fig. 10 shows the effect of the volume concentration on the relative thermal conductivity. As seen in Fig. 6, the infinite-shear thermal conductivity (k_∞) linearly increases with the volume concentration for a given particle size, whereas k_∞ proportionally increases with the 1.2th power of (d/D) as shown in Fig. 10. Combining these two parameters, a correlation for k_∞ is obtained as follows:

$$\frac{k_\infty}{k_L} = 1 + 0.46\left[\Phi\left(\frac{d}{D}\right)^{1.2}\right] \tag{8}$$

Based upon the above discussion and correlation, the present study proposes a new shear-rate-dependent thermal conductivity model of suspensions as follows:

$$\frac{k - k_0}{k_\infty - k_0} = 1 - \exp\left[\frac{C_3(\dot{\gamma} - \dot{\gamma}_0)}{\Phi^{0.8}(d/D)^{1.2}}\right] \tag{9}$$

where $C_3 = 14.28 \times 10^{-6}$ and Φ is the particle volume concentration. The proposed correlation can describe the shear rate dependence of thermal conductivity including the effects of volume concentration and particle size. Also, the correlation is able to describe the infinite-shear thermal conductivity. Fig. 11 shows the proposed correlation curve with the present experimental data. In Fig. 11, the normalized thermal conduc-

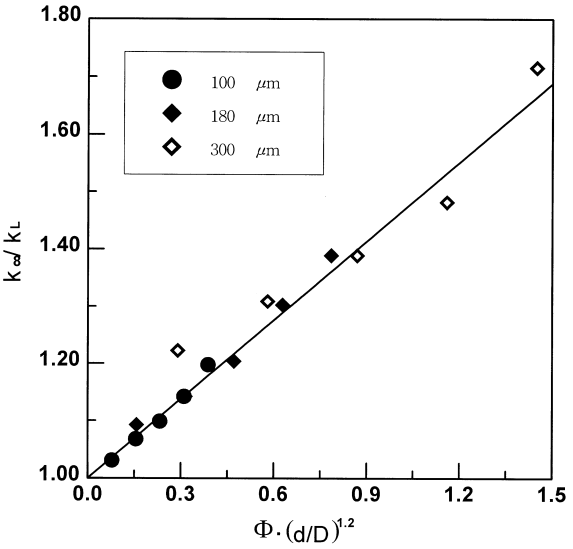

Fig. 10. Relative infinite-shear thermal conductivity vs. the abscissa $(\Phi)\ (d/D)^{1.2}$.

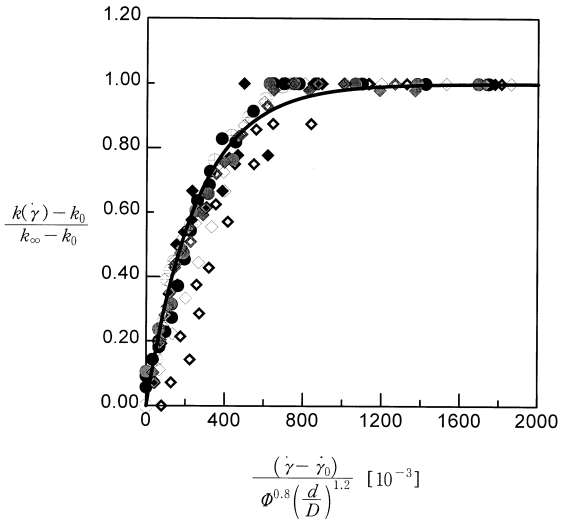

Fig. 11. Normalized thermal conductivity of suspensions as fitted by the proposed Eq. (9).

tivity of suspensions from experimental results shows a fair agreement with the proposed Eq. (9).

5. Summary and conclusions

The present study experimentally investigated the viscosity and thermal conductivity of the plastic particle suspensions. In particular, the shear rate dependence of the thermal conductivity was studied. Highly concentrated dispersions made of small size particles (25 μm) show a weak shear-thinning viscosity, whereas the low concentrated dispersions made of larger than 25 μm show nearly shear-rate-independent viscosity. However, it was found that for the suspensions of large particles ($d \geq 100$ μm), the thermal conductivity increased with shear rate, implying that the thermal conductivity is strongly dependent on the size of the dispersed particles. A shear-rate-dependence of thermal conductivity is increased with volume concentration. In addition, plateau values of the thermal conductivity were observed at relatively high shear rates for all test suspensions. The present study proposes a new correlation for shear-rate-dependent thermal conductivity of suspensions. This proposed model could be used in the numerical modeling of the heat transfer characteristics involving suspensions in a shear flow.

Acknowledgements

This research was sponsored by Korea Research Foundation (KRF. grant no. 1998-01-E00018). The authors wish to express their appreciation to KRF. In addition, the authors acknowledge useful discussion with Dr. Y. Cho at Drexel University.

References

[1] H.A. Barnes, J.F. Hutton, K. Walters, An Introduction to Rheology, Elsevier Science, New York, 1989.
[2] R. Furth, A.D. Cowper, Investigations on the Theory of the Brownian Movement by A. Einstein, Dover, New York, 1956.
[3] G.K. Batchelor, The effect of Brownian motion on the bulk stress in a suspension of spherical particles, J. Fluid Mechanics 83 (1977) 97–117.
[4] D.J. Jeffrey, A. Acrivos, The rheological properties of suspensions of rigid particles, AIChE J. 22 (1977) 417–432.
[5] A.S. Ahuja, Augmentation of heat transport in laminar flow of polystyrene suspensions: I. Experiments and Results, J. Applied Physics 46 (1975) 3408–3416.
[6] C.W. Sohn, M.M. Chen, Microconvective thermal conductivity in disperse two-phase mixtures as observed in a low velocity Couette flow experiment, Int. J. Heat Transfer 103 (1981) 47–51.
[7] C.W. Sohn, M.M. Chen, Heat transfer enhancement in laminar slurry pipe flows with power law thermal conductivities, J. Offshore Mechanics and Arctic Eng. 106 (1984) 539–542.
[8] P. Charunyakorn, S. Sengupta, S.K. Roy, Forced convection heat transfer in microencapsulated phase change material slurries: flow in circular ducts, Int. J. Heat Mass Transfer 34 (1991) 819–834.
[9] D.Y. Lee, T.F. Irvine, Shear rate dependent thermal conductivity measurements of non-Newtonian fluids, Experimental Thermal and Fluid Science 15 (1997) 16–24.
[10] E.R.G. Eckert, W.O. Carlson, Natural convection in an air layer enclosed between two vertical plates with different temperatures, Int. J. Heat Mass Transfer 2 (1961) 106–114.
[11] E. Elder, Laminar free convection in vertical slots, J. Fluid Mechanics 23 (1965) 77–87.
[12] S.H. Lee, Thermal conductivity measurements of suspensions in a shear field, M.S. thesis, Kyungpook National University, Korea, 1998.
[13] L. Haar, J.S. Gallagher, G.S. Kell, NBS/NRC Steam Tables: Thermodynamics and Transport Properties and Compute Programs for Vapor and Liquid States of Water in SI Units, McGraw-Hill, New York, 1984.
[14] A.D. Brailsford, K.G. Major, The thermal conductivity of aggregates of several phases including porous materials, J. Appl. Physics 15 (1964) 313–319.
[15] K. Litchnecker, The electrical conductivity of periodic and random aggregates, Physik, X 27 (1926) 115–120.